Late Neoproterozoic proto-arc ocean crust in the Dariv Range, Western Mongolia: a supra-subduction zone end-member ophiolite

ARJAN H. DIJKSTRA[1,2], FRAUKJE M. BROUWER[3], W. DICKSON CUNNINGHAM[4], CRAIG BUCHAN[1], GOMBOSUREN BADARCH[5] & PAUL R. D. MASON[6]

[1]*Tectonics Special Research Centre, Curtin University of Technology, GPO Box U 1987, Perth, WA 6845, Australia*

[2]*Present address: Institut de Géologie, Université de Neuchâtel, Rue Emile-Argand 11, CP2, CH 2007, Neuchâtel, Switzerland (e-mail: a.dijkstra@geosciencenet.com)*

[3]*Faculteit der Aard- en Levenswetenschappen, Vrije Universiteit, 1081 HV Amsterdam, The Netherlands*

[4]*Orogenic Processes Group, Department of Geology, University of Leicester, Leicester LE1 7RH, UK*

[5]*Institute of Geology and Mineral Resources, Mongolian Academy of Sciences, Ulanbaatar, Mongolia*

[6]*Vening Meinesz Research School Of Geodynamics, Faculteit Aardwetenschappen, Universiteit Utrecht, Budapestlaan 4, 3584 CD Utrecht, The Netherlands*

Abstract: An unusual late Neoproterozoic (*c.* 572 Ma) ophiolite is exposed in the Dariv Range (western Mongolia), which contains intermediate to acidic lavas and sheeted dykes, and an igneous layered complex consisting of gabbro–norites, websterites, orthopyroxenites and dunites underlain by serpentinized mantle harzburgites. Based on the compositions of the crustal units and the crystallization sequences in the mafic and ultramafic cumulates we conclude that the entire oceanic crust, including the cumulates, was made from arc magmas with boninitic characteristics. The Dariv rocks bear a strong resemblance to rocks recovered from the modern Izu–Bonin–Mariana fore-arc, a fragment of proto-arc oceanic basement, and we propose that the Dariv Ophiolite originated in a similar tectonic setting. A metamorphic complex consisting of amphibolite- to granulite-facies metasedimentary and meta-igneous rocks was thrust over the ophiolite. This metamorphic complex probably represents a Cambrian arc. Thrusting started before 514.7 ± 7.6 Ma as constrained by new sensitive high-resolution ion microprobe U–Pb zircon analyses from a syn- to post-tectonic diorite. The Dariv Ophiolite is a type-example of a proto-arc ophiolite, a special class of supra-subduction zone ophiolites.

Ever since ophiolites were recognized as fragments of oceanic lithosphere exposed within continental crust, it has been debated whether they represent 'normal' ocean floor created at mid-ocean ridges, or supra-subduction zone oceanic basement from fore-arc, proto-arc or back-arc basins (Miyashiro 1975; Coleman 1984; Nicolas 1989). Indeed, it has been found that many ophiolite complexes contain rocks (generally lavas and dykes) with geochemical characteristics that are typical of modern supra-subduction zone environments and that have been used as a 'supra-subduction zone signature' (Miyashiro 1973; Noiret *et al*. 1981; Pearce *et al*. 1981; Elthon 1991). However, a geochemical supra-subduction zone signature has also been found in volcanic rocks from the modern Chile Ridge, which is part of the Nazca–Antarctic plate subducted below the Andean margin (Klein & Karsten 1995), suggesting that this signature alone is not conclusive evidence for a supra-subduction zone origin. Therefore, other evidence besides the geochemistry of the rocks must be taken into account before a tectonic setting can be attributed. This includes evidence from field relations and regional geology for an association with arc-derived igneous and sedimentary rocks of similar age. Also, geochemical and petrological analysis should be conducted on all (exposed) crustal units, including igneous cumulates, to determine how widespread the supra-subduction zone characteristics are.

In this paper, we apply such an integrated approach to the not widely known Neoproterozoic Dariv Ophiolite of Western Mongolia. From previous work (e.g. Khain *et al*. 2003; B. F. Windley, pers. comm.) it was clear that this ophiolite was a candidate supra-subduction zone ophiolite. We report combined field, petrological and geochemical observations that strongly support a supra-subduction zone, probably proto-arc, origin. We have found that all the exposed crustal units (lavas, dykes and cumulates) crystallized from arc magmas with boninitic characteristics and their derivatives. The regional geology of the Dariv Range is consistent with the ophiolite having formed as proto-arc ocean floor. Together with a few other ophiolites with similar characteristics, Dariv represents the proto-arc end-member of the broader, more loosely defined supra-subduction zone ophiolite type, providing a reference point for comparison of other proposed supra-subduction zone ophiolites.

Geological context

The Central Asian Orogenic Belt is a classic accretionary orogen comprising a tectonic collage of subduction complexes, island arcs, ophiolites, and small continental fragments, accreted to the Siberian Craton during the Proterozoic and Palaeozoic (Sengör *et al*. 1993, 1994; Buslov *et al*. 2001; Khain *et al*. 2003). Central Asian Orogenic Belt rocks are well exposed in western Mongolia, especially in the Altai Mountains and neighbouring ranges (Fig. 1). The present-day topography of the Altai region is primarily brought about by Cenozoic transpression as the result of far-field stresses associated with the India–Eurasia collision (Cunningham *et al*. 1996, 2003). One of the areas uplifted during this deformation is the Dariv Range, a triangular massif bounded to the south by a prominent transpressional fault system of
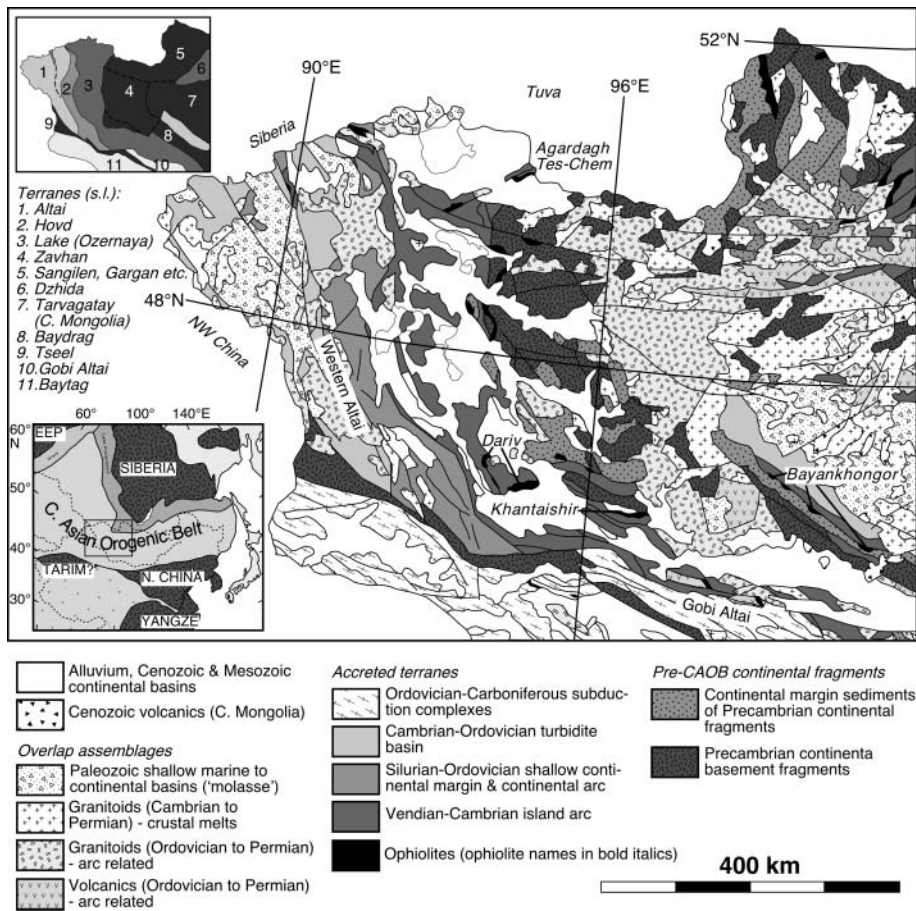
Fig. 1. Terrane map of western Mongolia. Modified from Dorjnamjaa *et al.* (1998) and Badarch *et al.* (2002). The main ophiolite complexes within the region discussed in the text are indicated. Inset at lower left shows the extent of the Central Asian Orogenic Belt within Asia.

Cenozoic age (Fig. 2a). The massif is surrounded by intermontane basins containing late Mesozoic and Cenozoic sediments showing classic inversion structures (Cunningham *et al.* 2003; Howard *et al.* 2003).

The Dariv Range straddles the terrane boundary between the Lake (or Ozernaya) terrane, which comprises Vendian–Early Palaeozoic island arc rocks, and the Zavhan terrane, a Precambrian micro-continent (Fig. 1; Sengör *et al.* 1993, 1994; Badarch *et al.* 2002). Previous work has shown that the Dariv Range consists of amphibolite- to granulite-facies meta-igneous and metasedimentary basement (the Dariv Metamorphic Complex), the Dariv Ophiolite complex (also named the Bayannur Ophiolite, Khain *et al.* 2003), and weakly metamorphosed igneous, sedimentary and volcanic rocks that are generally thought of as part of the Lake Terrane (Makarychev *et al.* 1986; Khain 1989). The Dariv Metamorphic Complex has been variably interpreted as Precambrian Zavhan basement (Makarychev *et al.* 1986), or a Cambrian island arc (Kozakov *et al.* 2002). The age of the Dariv Ophiolite is established by conventional U–Pb dating of zircon fractions from a plagiogranite, which yielded crystallization ages of 571 ± 4 and 573 ± 6 Ma (Table 1; Kozakov *et al.* 2002; Khain *et al.* 2003).

Results

The structure of the Dariv Range

We have made detailed geological transects in a small study area in the northwestern part of the Dariv Range, through the Dariv Ophiolite and through the neighbouring units to the south.

In addition, we have made a regional-scale map of the Dariv Range on the basis of an analysis of Landsat 5 (this is available online at http://www.geolsoc.org.uk/SUP18236; a hard copy can be obtained from the Society Library) and Aster satellite imagery, supplemented with information from published maps of Makarychev *et al.* (1986) and Khain *et al.* (2003) and from anonymous unpublished maps made by Mongolian workers.

Our fieldwork has shown that the study area consists of a stack of steeply south-dipping thrust sheets. The ophiolite complex is the lowermost thrust sheet in the area. The ophiolite is tectonically overlain by a sequence of strongly deformed metasedimentary and meta-igneous rocks. Our sections do not extend far enough to the south, into the core of the Dariv Range, to allow us to directly correlate these rocks with the high-grade rocks of the Dariv Metamorphic Complex described by other workers (Kozakov *et al.* 2002; Khain *et al.* 2003). On the basis of their high metamorphic grade, however, we group these rocks with the Dariv Metamorphic Complex. The structurally lowest of these metamorphic rocks consist of strongly deformed, isoclinally folded, foliated and locally lineated metacarbonates, serpentinite slivers, and psammitic and sillimanite-bearing pelitic paragneisses, which have recorded upper amphibolite-facies metamorphism coeval with thrusting. South of the study area, higher in the tectonic stack, they grade into amphibolite- to granulite-facies granodioritic to tonalitic orthogneisses, schists, and paragneisses. The sequence is intruded by syn- to post-tectonic quartz dioritic and gabbroic intrusions. Most rocks show evidence for dominant coaxial deformation, with intense tight to isoclinal, symmetric folding. Locally, protomylonites and mylonites record-
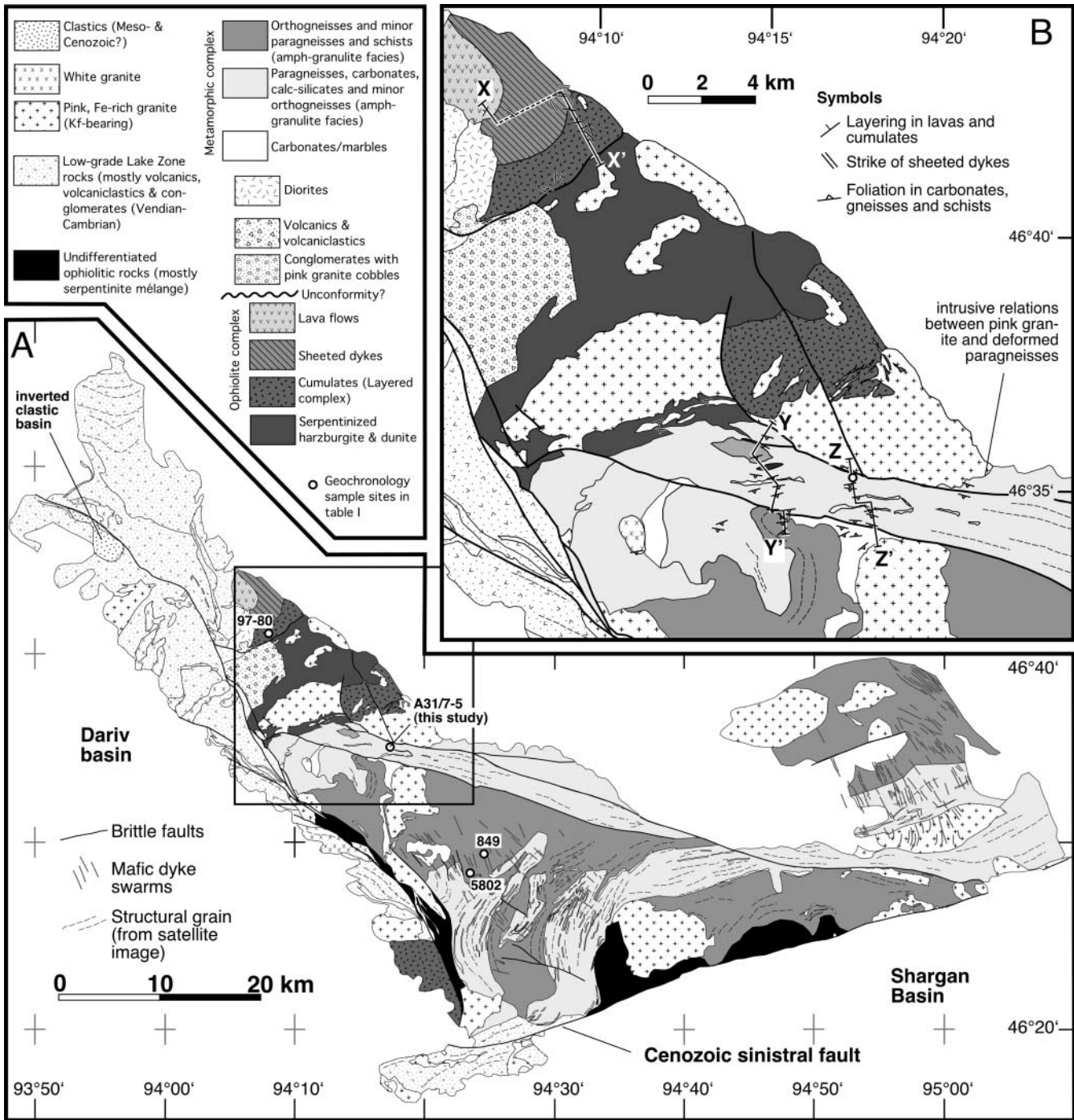
Fig. 2. Overview map of the Dariv Range. Map drawn in ARCVIEW on the basis of Landsat 5 and Aster satellite images and on our own mapping, published maps of Makarychev *et al.* (1986) and Khain *et al.* (2003), and anonymous unpublished maps of Mongolian workers. Geodetic projection with equal north–south and east–west scales. Inset shows detail map of the field study area in which ophiolitic rocks are exposed.

ing non-coaxial deformation have developed, predominantly in meta-igneous rocks (Fig. 3, sections Y and Z). Lineations and shear-sense indicators (asymmetric clasts, S–C fabrics and extensional crenulation cleavages) in these mylonitic rocks suggest north- to NW-directed (thrust) transport of the metamorphic complex over the ophiolite.

All units contain numerous pink granites, aplites, and plagio-clase–amphibole-phyric dykes that post-date the thrusting. At

least two prominent WNW–ESE- and NW–SE-trending brittle–ductile fault zones that post-date the intrusion of the pink granites cut across the studied sequence. These fault zones are locally associated with abundant pseudotachylytes. At several locations, carbonate rocks from adjacent units have been remobilized into the fault zones. In the satellite imagery there is evidence that these faults offset stratigraphic markers and rock complexes in a dextral fashion, and we conclude that these faults

Table 1. *Zircon ages from Dariv Range*

Sample	Location	Method	Age (Ma)	Significance	Reference
Plagiogranite (sample 97-80) within ophiolite	Northern ophiolite complex (Fig. 2)	U–Pb TIMS	571 ± 4	Emplacement, proto-arc spreading	Khain *et al.* (2003); Kozakov *et al.* (2002)
			573 ± 6		
Dioritic gneiss	Not reported	Pb–Pb evaporation	1426.4 ± 1.2	Emplacement	Kröner *et al.* (2001)
Garnet–hypersthene granulite gneiss (sample 849)	Metamorphic complex (Fig. 2)	U–Pb TIMS	1360 ± 56	Upper intercept, inherited	Kozakov *et al.* (2002)
			510 ± 4	Lower intercept, metamorphism	
Gneissose bt–hbl tonalite body within migmatites (sample 5802)	Metamorphic complex (Fig. 2)	U–Pb TIMS	1630 ± 159	Upper intercept, inherited	Kozakov *et al.* (2002)
			490 ± 4	Lower intercept, emplacement, syn-metamorphism	
Qtz diorite (sample A31/7-5)	Metamorphic complex, *c.* 100 m S of 46°35.232′N, 94°17.276′E	U–Pb SHRIMP	2452 ± 5	Xenocryst	This study
			794.3 ± 13.5	Xenocryst	
			514.7 ± 7.6	Pooled age, emplacement, syn-accretion	
Undeformed volcanic sandstone unconformably overlying ophiolite	Not reported	Pb–Pb evaporation	497.6 ± 1.0	Uniform detrital zircon population, maximum deposition age	Kröner *et al.* (2001)
Conglomerate from volcanic arc association in tectonic contact with ophiolite	Not reported	Pb–Pb evaporation	539.7 ± 1.0	Qtz porphyry clast	Kröner *et al.* (2001)
			492.0 ± 1.0	Granite clast, maximum deposition age	
Pink stitching granite between ophiolite and arc association	Not reported	Pb–Pb evaporation	497.5 ± 1.0	Emplacement, post-accretion	Kröner *et al.* (2001)

TIMS, thermal ionization mass spectrometry.

probably had a dextral strike-slip component of deformation. One of these faults runs along the southern margin of a kilometre-scale pink granite pluton in the study area, and in places the granite is deformed into an augen-gneiss along this margin, locally obscuring the intrusive relation of the granite into the deformed metamorphic rocks of the Dariv Metamorphic Complex. In the southwestern quadrant of our study area, intrusive relations between the granite pluton and deformed rocks of the Dariv Metamorphic Complex are preserved (Fig. 2b). In the SW of the study area, the ophiolitic and metasedimentary and meta-igneous thrust sheets are juxtaposed against largely un-metamorphosed rocks of the Lake Terrane by steep, NW–SE-striking faults of unknown age. These Lake Zone rocks comprise conglomerates, volcanic, plutonic and volcaniclastic rocks, as well as slivers of serpentinite (Makarychev *et al.* 1986). The satellite images show that one of the NW–SE-trending faults is associated with an inverted continental clastic (Mesozoic–Cenozoic) basin in the north of the Dariv Range (Fig. 2a), and we suggest that the NW–SE-trending faults have recorded Cenozoic transpression associated with the uplift of the Dariv Range and adjacent ranges in western Mongolia.

New geochronological constraints on the age of the thrusting

We have sampled an undeformed quartz diorite (Fig. 4a) from the metamorphic units immediately overlying the ophiolite for U–Pb sensitive high-resolution ion microprobe (SHRIMP) zircon dating at Curtin University. Identical diorites are often sheared within the same sequence, and we interpret these intrusions as syn- to post-tectonic. We also measured the whole-rock major and trace element composition of this dioritic sample using inductively coupled plasma atomic emission spectrometry (ICP-AES) and inductively coupled plasma mass spectrometry (ICP-MS) at the Department of Applied Chemistry at Curtin University (data are available as a Supplementary Publication; see p. 000). The diorite is a low-Fe ($FeO^*/Mg = 2.0$), high-K (3.6 wt% K_2O) subalkaline rock (Arculus 2003), plotting close to the tholeiitic–calcalkalic boundary of Kuno (1968) in terms of its alkali, FeO, and MgO (AFM) components. It is strongly enriched in large ion lithophile elements (LILE) and light rare earth elements (REE), and shows prominent negative Nb and Ti anomalies and a positive Pb anomaly with respect to neighbouring trace elements with similar bulk compatibilities in the primitive mantle normalized trace element diagram in Figure 4c.

Zircons were extracted from this diorite by standard crushing, milling, sieving, heavy liquid, and magnetic separation techniques at the NERC Isotope Geosciences Laboratory, Keyworth (UK). Zircons were generally colourless and small, <200 μm, with euhedral to slightly rounded crystal shapes. A representative selection of zircons was handpicked, and mounted in epoxy together with chips of CZ3 zircon standard. Cathodoluminescence (CL) images were obtained with a Philips XL30 SEM. Zircons show clear oscillatory zoning in the CL images (Fig.
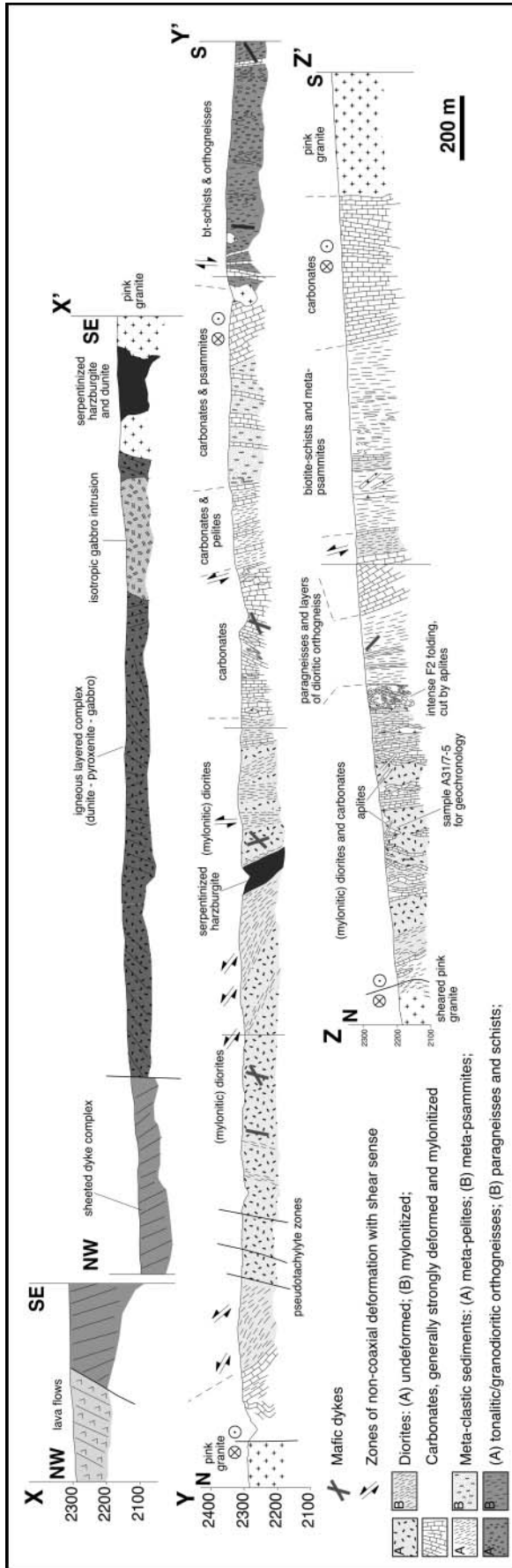
Fig. 3. Cross-sections (no vertical exaggeration) across the Dariv Ophiolite and the metamorphic complex, based on our mapping. Fill patterns for ophiolitic units are the same as in Figure 2. Locations are shown in inset map in Figure 2.

4b). We obtained a concordia age for 10 individual concordant zircon analyses (Fig. 4d; see also the Supplementary Publication, see p. 364) of 514.7 ± 7.6 Ma (error quoted at 95% confidence level), which we interpret as the crystallization age of the diorite. Two zircons that gave young (<490 Ma) $^{206}Pb/^{238}U$ ages, one of which also had high common Pb, had probably suffered a post-crystallization Pb loss event and were excluded. Two zircons had cores that gave older ages of 2462 and 795 Ma (Fig. 4b and d), and we interpret these zircons as xenocrysts. The zircons, including the xenocrysts, had $^{232}Th/^{238}U$ ratios of 0.2–0.7, in agreement with a magmatic origin. Based on the crystallization age of the diorite, we conclude that thrusting of the metamorphic complex over the ophiolite (and associated magmatism and metamorphism) occurred during the Early–Mid-Cambrian.

Petrological and geochemical characteristics of the Dariv Ophiolite

In the north of the study area, a relatively complete ophiolitic sequence is present (Figs 2 and 3). This sequence consists of (from top to bottom) a series of lava flows, a sheeted dyke complex, an igneous layered complex, and serpentinized harzburgites and dunites. The contacts between the units are tectonic in character. The orientations of the lava flows, sheeted dykes, and cumulate layering are all consistent with an ophiolite sequence with a palaeo-horizontal that is now dipping steeply towards the NW. We measured whole-rock major and trace element concentrations of two lava and five dyke samples using X-ray fluorescence (XRF) at the Department of Geology at the University of Leicester (data are available as a Supplementary Publication; see p. 364). We also obtained solution ICP-MS trace element compositions of whole-rock powders of the two freshest dyke samples (see the Supplementary Publication; analyses were carried out at the Department of Applied Chemistry at Curtin University). In addition, we determined trace element concentrations in clinopyroxenes in two polished sections of samples of layered gabbro from the igneous complex by *in situ* laser ablation (LA) ICP-MS at Utrecht University (see the Supplementary Publication). These analyses are used to constrain the composition of the melts in equilibrium with the cumulates, and to investigate whether lavas, dykes, and gabbros are co-magmatic.

Lava flows

A series of lava flows and sills of 50 cm to 10 m thickness forms the uppermost ophiolite unit. These lavas consist of vesicular aphyric to plagioclase-phyric basalts (Fig. 5c), and orange andesites containing phenocrysts of plagioclase, and amphibole. We have not found pillow lavas as part of the ophiolite sequence exposed in the study area. Based on whole-rock chemical analyses of two samples these lavas are classified as trachy-basalts and trachy-andesites. They are enriched in LILE with respect to middle REE (MREE) and heavy REE (HREE) and transition metals in the primitive mantle-normalized trace element diagrams of Figure 6a and b. The lavas display pronounced negative Nb and Ti, and positive Pb anomalies with respect to neighbouring elements in the trace element diagram.

Sheeted dykes

The sheeted dyke complex consists of metre-scale mutually intrusive dykes (Fig. 5a), ranging in composition from basaltic andesites to rhyolites. In the study area, the contact with overlying lava flows is formed by an unexposed fault, but the
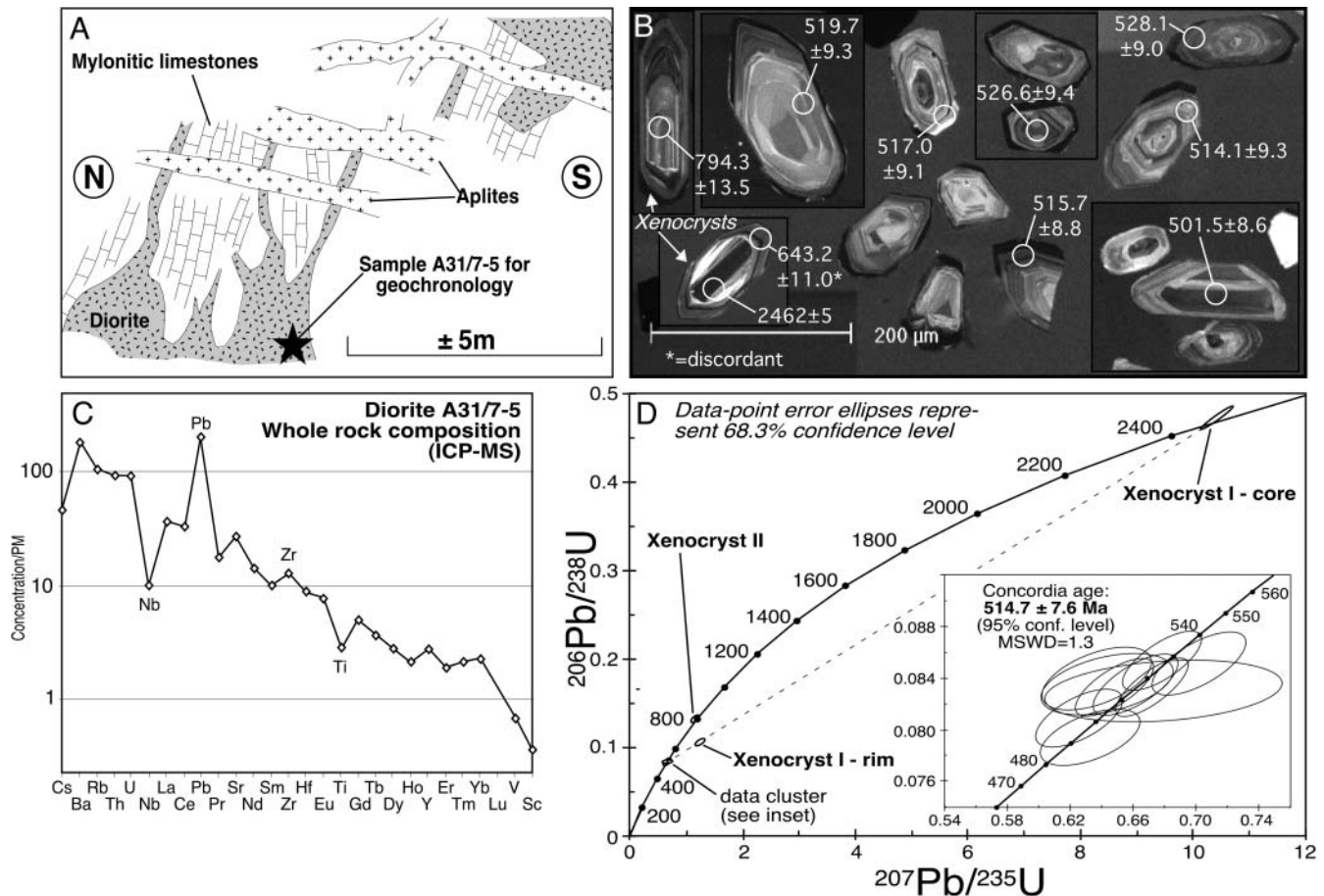
Fig. 4. (**a**) Sketch showing field relations between quartz diorite A31/7-5 sampled for geochronology and surrounding rocks. The diorite is interpreted as syn- to post-tectonic. Location of sample is shown in Figure 3. (**b**) Cathodoluminescence (CL) images of selected zircons and their ages determined by SHRIMP, showing magmatic oscillatory and sector zoning in most zircons, with some recrystallization of core regions. (**c**) Trace element diagram showing whole-rock composition of the analysed quartz diorite normalized to primitive mantle (PM; McDonough & Sun 1995). (**d**) Concordia diagram showing individual U–Pb isotope analyses with 1σ error ellipses obtained by SHRIMP at Curtin University. The data were processed using SQUID v.1.06 and ISOPLOT v.2.49 (Ludwig 2001*a*, *b*). One xenocrystic zircon had a core of 2452 Ma (Pb–Pb) and a discordant rim that was probably in part reset by the host magma. Inset shows detail of the concordia. Quoted weighted mean age of the concordant analyses has a confidence level of 95%.

orthogonal orientations of dykes and lavas suggest that rotations between the two units were minimal. The basaltic andesite dykes contain phenocrysts of plagioclase and augite in a plagioclase groundmass (Fig. 5d). The acidic dykes are equigranular, consisting of plagioclase, magmatic amphibole and (intercumulus) quartz (Fig. 5e). The chemical compositions of the two basaltic andesite dykes analysed strongly resemble those of boninites (Fig. 6a and b): they have a high SiO_2 at given MgO content, low TiO_2 (0.4%) and Zr (38–45 ppm, Ti/Zr <60), and high Cr (190–380 ppm) and Ni (60–100 ppm), but they are too evolved (<7 wt% MgO, no orthopyroxene) to be classified as true boninites (see Hickey & Frey 1982; Taylor *et al*. 1994). The whole-rock trace element patterns mimic those of the lavas, with LILE enrichment and negative Nb and positive Pb anomalies, although trace element concentrations are generally lower in the dykes (Fig. 6a). Even though the rocks are fractionated, the concentrations of the most compatible elements (e.g. the HREE) are depleted with respect to normal mid-ocean ridge basalt (N-MORB). This is also a typical feature of boninites, indicating derivation from a relatively refractory mantle source (Taylor *et al*. 1994).

Igneous layered complex

An igneous layered complex of mafic and ultramafic cumulates (Fig. 5b) underlies the dykes, with the actual contact marked by a brittle fault. The presence of numerous dykes similar in orientation and composition to those in the sheeted dyke complex suggests that the units are related, with no more than a limited part of the sequence missing. The layered complex consists of an association of generally concordant units of (from bottom to top) dunites with chromite seams (olivine + chromite), orthopyroxenites (olivine + orthopyroxene), websterites (ortho-pyroxene + clinopyroxene) and gabbro–norites (clinopyroxene ± orthopyroxene + plagioclase, Fig. 5b and f). Individual units range in thickness from one to several tens of metres, and websterite–norite packages are dominant at the top of the section, whereas cumulate dunite–orthopyroxenite packages are more typical for the base of the sequence. Based on these field relations and on petrographic analysis of individual samples with cumulate textures (e.g. Fig. 5f), the crystallization sequence in these rocks is interpreted as olivine + chromite → orthopyroxene → clinopyroxene → plagioclase.

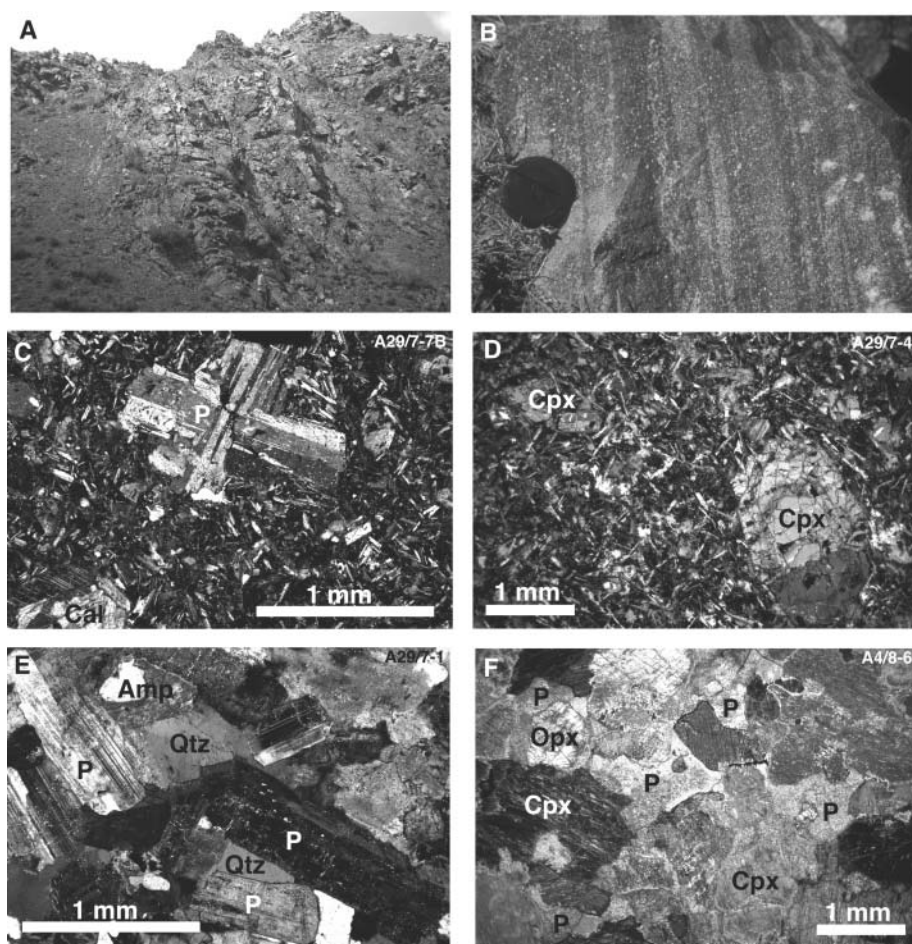The trace element composition of clinopyroxenes from two

Fig. 5. Field photographs and photomicrographs of ophiolitic rocks from Dariv. All photomicrographs taken with crossed polars. P, plagioclase; Cal, calcite; Cpx, clinopyroxene; Amp, amphibole; Qtz, quartz; Opx, orthopyroxene. (**a**) Sheeted dyke complex with person for scale. Dykes dip steeply to the right (NE). (**b**) Layered noritic gabbro, consisting of varying modal proportions of clinopyroxene, minor orthopyroxene and plagioclase. (**c**) Photomicrograph of plagioclase-phyric basaltic lava. (**d**) Basaltic andesite dyke from sheeted dyke complex, containing augite phenocrysts in a plagioclase–clinopyroxene groundmass. (**e**) Dacitic dyke with equigranular microgabbroic texture, containing amphibole, plagioclase and intercumulus quartz. (**f**) Gabbro–norite containing clinopyroxene and orthopyroxene and intercumulus altered plagioclase.

noritic layered gabbros was determined by LA-ICP-MS (Fig. 6c). From these compositions we have calculated equilibrium melt compositions (Fig. 6d), using an internally consistent set of partition coefficients based on the measured coefficients of Hauri *et al*. (1994). More details of the method are given in the caption of Figure 6. The modelled trace element pattern for the elements Th to V of the equilibrium melt agrees well with that of the whole-rock analyses of dykes and lavas, with negative Nb and positive Pb anomalies (Fig. 6d). Calculated Ba, Rb and Pb concentrations in the equilibrium melt are too high compared with concentrations in the dykes. This discrepancy in the most incompatible and mobile elements may be caused by microscopic alteration products, by the presence of a small trapped melt component in the cumulate clinopyroxenes (Bédard 1994), by chemical re-equilibration during post-cumulus melt percolation (e.g. chromatographic effects, Navon & Stolper 1987), or by an underestimation of clinopyroxene–melt partition coefficients for these elements.

Serpentinites

The lowermost ultramafic cumulates grade downward into serpentinites that are interpreted as altered residual mantle rocks of harzburgitic and dunitic composition. We have not found relict olivine in any of the serpentinite samples collected. Orthopyroxene is generally retrogressed to bastite assemblages, although small orthopyroxene relics remain. We have found no clinopyroxene. Spinel is often preserved and is opaque as a result of its high Cr content.

Other rocks associated with the ophiolite

Isotropic gabbro plutons ranging in size from several tens of metres to several hundreds of metres are found within the layered complex and within the peridotites. A kilometre-sized two-pyroxene gabbro pluton is found within serpentinized peridotites in the southeastern part of the ophiolite complex (Fig. 2b). Other late-stage intrusive rocks within the ophiolite sequence are quartz diorites, pink granites and generally NW−SE-striking plagioclase–amphibole-phyric dykes that form dyke swarms in places (Fig. 2a). We also encountered weakly deformed volcanic and volcaniclastic rocks, as well as matrix-supported red conglomerates, in tectonic contact with ophiolitic rocks. The presence of cobble-sized fragments of the very distinctive pink granite within the conglomerates indicates that these rocks are significantly younger than the ophiolite, the Dariv Metamorphic Complex, and the late-stage granites.

Discussion

An arc−proto-arc pair

Our mapping has shown that foliations, axial planes and shear zones in the Dariv Metamorphic Complex sequence are predominantly vertical to south-dipping, and that lineations and shear-sense indicators in non-coaxially deformed rocks found in the study area indicate top-to-the-north directed transport. The presence of serpentinite slivers amongst mylonitic diorites (Fig. 3, section Y) within the deformed sequence suggests tectonic
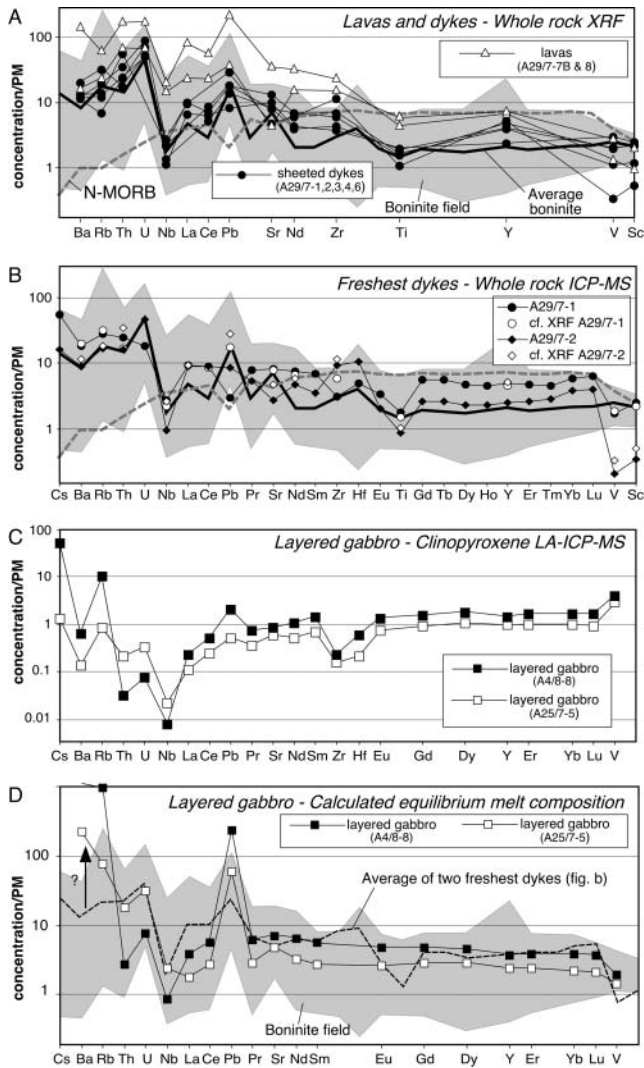
Fig. 6. Geochemistry of ophiolitic rocks. (**a**) Whole-rock XRF analyses for two lavas and five dykes, normalized to primitive mantle concentrations of McDonough & Sun (1995). Compositions are compared with N-MORB (Sun & McDonough 1989) and with average boninite and boninite field derived from precompiled boninite database from GEOROC (http://georoc.mpch-mainz.gwdg.de/georoc), and from Hickey & Frey (1982) and Taylor *et al*. (1994). (**b**) Whole-rock ICP-MS analyses for the two freshest (and most fractionated) dykes. The values determined by XRF for these same dykes are shown for comparison; these values agree well for most elements except Pb and Zr. Boninite field and average boninite and N-MORB compositions as in (**a**). (**c**) Average trace element compositions of clinopyroxene from two layered clinopyroxene–orthopyroxene–plagioclase gabbros from the layered complex obtained by LA-ICP-MS (Mason *et al*. 1999), normalized to primitive mantle. (**d**) Compositions of calculated melt compositions in equilibrium with clinopyroxenes, normalized to primitive mantle. Solid–melt partition coefficients used (for data see Supplementary Publication; see p. 364) are based on those of Hauri *et al*. (1994), except for Rb, which is based on McKenzie & O'Nions (1991). Partition coefficients for trivalent cations were adjusted to fit the elastic lattice strain model of Blundy & Wood (1994) and Wood & Blundy (1997). The partition coefficients for Zr and Hf from Hauri (1994) yielded depletions for these elements in the equilibrium melt with respect to neighbouring elements, which is inconsistent with the whole-rock compositions of lavas and dykes. Melt compositions are compared with average of the two dykes from (**b**), and with the boninite field.

duplication, a feature that is consistent with thrusting. There is no evidence that the entire sequence is overturned: pseudostratigraphic relations in the ophiolite sequence are in agreement with a tilted, but non-overturned orientation. On the basis of these relations we conclude that the Dariv Metamorphic Complex was thrust northwards over the Dariv Ophiolite. This interpretation differs from that of Khain (1989) and Khain *et al*. (2003), who concluded that the ophiolite was thrust over the Dariv Metamorphic Complex. Our interpretation is in agreement, however, with the interpretation of Makarychev *et al*. (1986). Intrusion of diorite bodies occurred during and after the thrusting. After thrusting had ceased, the entire thrust sequence was intruded by pink (stitching) granites.

The Dariv Metamorphic Complex has previously been interpreted as a Precambrian continental fragment, possibly part of the Zavhan microcontinent (Makarychev *et al*. 1986; Khain 1989). Recent zircon dating by Kozakov *et al*. (2002), however, has shown that igneous protoliths and granulite-facies metamorphism, previously thought to have been Precambrian, were Early–Mid- to Late Cambrian in age, and that there are no reliable candidates for older basement in the area. It was therefore concluded that the Dariv Metamorphic Complex represents a Cambrian island arc (Kozakov *et al*. 2002). This suggests that the Dariv Metamorphic Complex may represent an equivalent to the Lake Zone island arc rocks that has been deformed and metamorphosed to high grade.

The chemical composition of the quartz diorite analysed in this study resembles that of modern-day island arcs, volcanic arcs and syncollisional granitoids. This and other similar diorites in the area that intrude the ophiolite and the Dariv Metamorphic Complex may therefore have been formed by arc magmatism, or by magmatism associated with arc accretion; the syn- to post-tectonic character supports the latter view. The two xenocrystic zircons in the diorite that we analysed may have been derived from the basement or sediments from the continental block onto which the arc was accreted, or from pre-existing continental crust in the arc basement. We note that the combination of *c*. 2.5 Ga and *c*. 800 Ma ages is common in basement of East (Madagascar, India) and West (Tanzania craton, Mozambique belt) Gondwanaland.

The petrological and geochemical characteristics of the ophiolitic complex support an arc environment. The crustal rocks of the Dariv Ophiolite show strong similarity to samples of oceanic basement from the modern-day Izu–Bonin–Mariana fore-arc. The similarities include intermediate-to-acidic compositions of dykes and lavas, low-Ti composition of lavas and dykes, enriched LILE and Pb but depleted Nb compositions of lavas, dykes and cumulates, and the evidence for early crystallization of orthopyroxene and late crystallization of plagioclase in the plutonic rocks (Bloomer & Hawkins 1983; Bloomer *et al*. 1995). The Izu–Bonin–Mariana fore-arc rocks were formed by oceanic spreading shortly after the initiation of subduction, before the establishment of the Mariana arc, and are therefore thought to represent infant- or proto-arc sea floor (Bloomer *et al*. 1995). Following uniformitarian principles, we propose that the Dariv Ophiolite represents oceanic proto-arc basement from a fore-arc (Fig. 7).

Clinopyroxenes in two cumulate gabbros from the igneous layered complex are in trace element equilibrium with a melt that closely resembles the melt from which the dykes and the lavas crystallized (Fig. 6d), suggesting that all units may be co-magmatic. The trace element patterns of the magmas that produced the Dariv lavas, dykes, and gabbros do not resemble those of mid-ocean ridge basalts; instead they correspond to those of boninite melts and their derivatives (Fig. 6a, b and d),
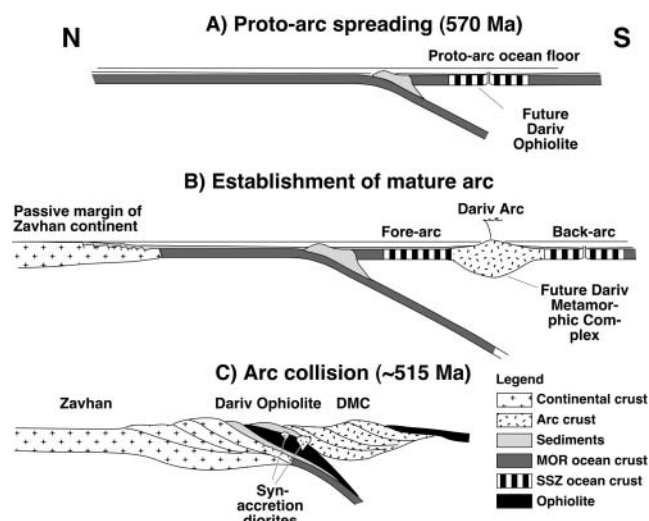
Fig. 7. Tectonic model for the formation and emplacement of the Dariv Ophiolite and the Dariv Metamorphic Complex (DMC), based on the reconstruction of the western Pacific and the emplacement of the Papua New Guinea Ophiolite (Milsom 2003). (**a**) Proto-arc spreading above an intra-oceanic subduction zone produces the future Dariv Ophiolite. (**b**) Establishment of a mature arc, the future Dariv Metamorphic Complex. (**c**) Arc-continent collision leads to stacking of the Dariv arc and associated fore–arc sediments onto the Dariv Ophiolite. SSZ, supra-subduction zone.

lending further support to their proposed origin in a proto-arc environment.

The structural relation between the arc and fore-arc complexes in Dariv suggests that they developed above a south-facing subduction zone (in the present-day reference frame), and that before 515 Ma the arc had started to be thrust over the fore-arc region. This probably occurred during accretion of the Dariv arc onto the Zavhan microcontinent (Fig. 7). Similar relations are found in the Bayankhongor region in Central Mongolia (Fig. 1), where a Vendian–Cambrian accretionary complex and Archaean–Proterozoic basement of the Baydrag block overthrust the c. 570 Ma Bayankhongor ophiolite, probably in a south-facing subduction zone environment (Buchan et al. 2001, 2002). These results are at odds with the model of Sengör et al. (1993, 1994) for the development of the Central Asian Orogenic Belt, which centres on the existence of a long-lived, north-facing subduction zone throughout the Neoproterozoic and Palaeozoic, above which fragments of the Palaeo-Asian ocean were accreted to the Siberian craton. Our observations confirm that accretionary orogenesis in the Central Asian Orogenic Belt may have involved subduction zone switches during discrete tectonic events associated with arc-accretion or with collision between microcontinental blocks, as proposed by Buchan et al. (2001, 2002).

Proto-arc and supra-subduction ophiolites

The Dariv Ophiolite is unusual because none of the rocks from the crustal sequence resemble mid-ocean ridge basalts in terms of petrology or geochemistry. Instead, parental melts of the crustal rocks, including the cumulates, resemble island arc tholeiites and boninites and their derivatives. Other ophiolites that also have these unusual characteristics occur within the Central Asian Orogenic Belt (e.g. the Khan Taishir and Agardagh

Table 2. *Comparison between proto-arc ophiolites and some classic ophiolites that are often referred to as supra-subduction zone ophiolites*

	Proto-arc end-member (Dariv or Betts Cove type)	Other supra-subduction zone assigned ophiolites*
Extrusive rocks	Intermediate–acidic arc tholeiitic and boninitic lavas with LILE and LREE enrichment, and Nb and Ti depletion	MORB lavas evolving to intermediate arc tholeiitic and boninitic lavas with LILE and LREE enrichment, and Nb and Ti depletion
Sheeted dykes	Intermediate–acidic–boninitic compositions with LILE and LREE enrichment, and Nb and Ti depletion	Generally MORB composition, with second generation dykes with arc tholeiite–boninite characteristics
High-level plutonic rocks	Hornblende–quartz gabbros and diorites	Isotropic gabbros with MORB-liquid compositions (non-cumulates); Fe–Ti-rich evolved gabbros
Low-level cumulates	Dunite–orthopyroxenite–websterite–gabbro–norite association derived from arc tholeiite magmas by crystal fractionation following the ol–opx–cpx–plag crystallization sequence	Dunite–troctolite–wehrlite–gabbro–norite association derived from MORB magmas by crystal fractionation following the ol–plag–cpx–opx crystallization sequence; local ol–cpx–opx–plag sequences (e.g. Vourinos)
Mantle rocks	Highly depleted harzburgites with Cr-number >0.6 spinel and highly depleted trace element patterns in cpx	Variably depleted lherzolites and harzburgites with a range of spinel compositions and cpx showing LREE depletion, as well as 'spoon-shaped' patterns with LREE enrichment
Intrusive rocks	Plagiogranites; hornblende–quartz gabbros and diorites	Wehrlites; plagiogranites; hornblende–quartz gabbros and diorites
Regional geology	Associated with volcaniclastic rocks and deep or shallow marine sediments; associated with arc complexes	Associated with cherts and other deep-marine sediments; in few cases associated with volcaniclastic rocks and arc complexes
Modern settings with similar rock associations	Proto-arc basement in Izu–Bonin–Mariana fore-arc (Bloomer & Hawkins 1983; Bloomer et al. 1985; Parkinson & Pearce 1998)	New Britain back-arc (Woodhead et al. 1998); Parece Vela back-arc (Ohara et al. 2003); Mariana back-arc (Ohara et al. 2002); Chile Ridge (Klein & Karsten 1995)
Selected examples and references	Dariv (Makarychev et al. 1986; Khain et al. 2003; this paper); Khan Taishir (Zonenshain & Kuzmin 1978; Matsumoto & Tomurtogoo, 2003); Agardagh Tes-Chem (Phänder et al. 2002); Trinity (Metcalf et al. 2000); Papua (England & Davies 1973); Betts Cove (Church 1977, 1979; Church & Riccio 1977; Bédard et al. 1998; Bédard 1999); Thetford Mines (Schroetter et al. 2003); Troodos? (Coogan et al. 2003).	Oman (Pearce et al. 1981; MacLeod & Yaouancq, 2000; Ishikawa et al. 2002); Bay of Islands (Elthon 1991; Varfalvy et al. 1996); Vourinos (Jackson et al. 1975; Noiret et al. 1981; Beccaluva et al. 1984); Pindos (Saccani & Photiades 2004); Xigaze (Griselin 2001); Donqiao (Girardeau et al. 1986); Sulawesi (Monnier et al. 1995); Zambales (Hawkins & Evans 1983).

*This category may include back-arc ophiolites, ophiolites with polygenetic mid-ocean ridge and supra-subduction zone histories, and ophiolites for which a supra-subduction zone origin is debated (e.g. Oman, see Boudier et al. 1997).

Tes−Chem ophiolites; Zonenshain & Kuzmin 1978; Pfänder *et al*. 2002). They are also found within other orogens around the world, with the Trinity, Papua, Betts Cove, and Thetford Mines ophiolites as some of the best known examples (see Table 2). Church (1977, 1979) recognized this distinct ophiolite type and referred to it as 'oceanic crust of the Betts Cove type' after the type-locality in Canada. Subsequent workers made the link between Betts Cove type ophiolites and boninitic ocean floor (e.g. Bédard *et al*. 1998; Bédard 1999). In most of these examples, ophiolites are closely associated with preserved arc complexes or arc-derived sediments of similar age. The Troodos Ophiolite has many characteristics, including crystallization sequences, that fit with a proto-arc origin, but this ophiolite is not associated with volcaniclastic or igneous rocks with an arc affinity (e.g. Coogan *et al*. 2003).

In contrast, evidence for an arc environment of origin is much weaker in some of the classic ophiolites that have been proposed to have originated in supra-subduction zone environments (e.g. Oman, Bay of Islands, Vourinos, Pindos). Clear geochemical evidence for a supra-subduction zone origin in these ophiolites is often restricted to an upper sequence of lavas (e.g. the 'V2 lavas' in Oman), and to a minor proportion of dykes. In the Bay of Islands ophiolite, there is evidence for magmas of boninitic affinity intruding mantle and lower crustal rocks (Bédard 1993; Varfalvy *et al*. 1996). However, in these examples the bulk of the plutonic sequences generally display the normal 'MORB' fractionation sequence olivine + chromite → plagioclase → clinopyroxene → orthopyroxene, leading to dunite−troctolite−wehrlite−gabbro−norite associations (Church & Riccio 1977). Such ophiolites may originate in back-arc basins, which generally consist of MORB-type oceanic basement with weak or absent supra-subduction zone signatures (e.g. Taylor *et al*. 1992; Monnier *et al*. 1995; Woodhead *et al*. 1998; Ohara *et al*. 2003). However, such ophiolites may also develop at a Chile Ridge-type oceanic spreading centre close to a subduction zone (Klein & Karsten 1995). Alternatively, they may represent mid-ocean ridge basement, later modified in a supra-subduction zone environment after the initiation of intra-oceanic subduction (see, e.g. Griselin 2001, for the Xigaze Ophiolite, Tibet). We thus argue that the environment of origin of these classic 'supra-subduction zone' ophiolites is not very well constrained, and that they cannot act as type examples of supra-subduction zone oceanic basement.

We conclude that the Dariv Ophiolite and several other 'atypical' ophiolites form a well-defined end-member ophiolite type that probably represents proto-arc ocean floor (Table 2). The most useful criteria for recognizing this proto-arc ophiolite type in the field are the prevalence of intermediate−acidic lavas and sheeted dykes, crystallization sequences in cumulates characterized by late crystallization of plagioclase (Church & Riccio 1977; Bloomer & Hawkins 1983), and regional geological evidence for association with arc-derived rocks. All these features taken together are strong evidence for a supra-subduction zone environment of origin.

References

ARCULUS, R.J. 2003. Use and abuse of the terms calcalkaline and calcalkalic. *Journal of Petrology*, **44**, 929–935.

BADARCH, G., CUNNINGHAM, W.D. & WINDLEY, B.F. 2002. A new terrane subdivision for Mongolia: implications for the Phanerozoic crustal growth of Central Asia. *Journal of Asian Earth Sciences*, **21**, 87–110.

BECCALUVA, L., OHNENSETTER, D., OHNENSETTER, M. & PAUPY, A. 1984. Two magmatic series with island arc affinities within the Vourinos ophiolite. *Contributions to Mineralogy and Petrology*, **85**, 253–271.

BÉDARD, J.H. 1993. The oceanic crust as a reactive filter: multiple syn-kinematic intrusion, hybridization and assimilation in an ophiolitic magma chamber. *Geology*, **21**, 77–80.

BÉDARD, J.H. 1994. A procedure for calculating the equilibrium distribution of trace elements among minerals of cumulate rocks, and the concentration of trace elements in coexisting liquids. *Chemical Geology*, **118**, 143–153.

BÉDARD, J.H. 1999. Petrogenesis of boninites from the Betts Cove ophiolite, Newfoundland, Canada: identification of subducted source components. *Journal of Petrology*, **40**, 1853–1889.

BÉDARD, J.H., LAUZIÈRE, K., TREMBLAY, A. & SANGSTER, A. 1998. Evidence for fore-arc seafloor spreading from the Betts Cove ophiolite, Newfoundland: oceanic crust of boninitic affinity. *Tectonophysics*, **284**, 233–245.

BLOOMER, S.H. & HAWKINS, J.W. 1983. Gabbroic and ultramafic rocks from the Mariana Trench: an island arc ophiolite. *In:* HAYES, D. (ed.) *The Tectonic and Geologic Evolution of Southeast Asian Seas and Islands, Part 2*. Geophysical Monograph, American Geophysical Union, **27**, 294–317.

BLOOMER, S.H., TAYLOR, B., MACLEOD, C.J., STERN, R.J., FRYER, P., HAWKINS, J.W. & JOHNSON, L. 1995. Early arc volcanism and the ophiolite problem: a perspective from drilling in the Western Pacific. *In:* TAYLOR, B. & NATLAND, J. (eds) *Active Margins and Marginal Basins of the Western Pacific*. Geophysical Monograph, American Geophysical Union, **88**, 1–30.

BLUNDY, J. & WOOD, B. 1994. Prediction of crystal−melt partition coefficients from elastic moduli. *Nature*, **372**, 452–454.

BOUDIER, F., NICOLAS, A., ILDEFONSE, B. & JOUSSELIN, D. 1997. EPR microplates, a model for the Oman Ophiolite. *Terra Nova*, **9**, 79–82.

BUCHAN, C., CUNNINGHAM, W.D., WINDLEY, B.F. & TOMURHUU, D. 2001. Structural and lithological characteristics of the Bayankhongor Ophiolite Zone, Central Mongolia. *Journal of the Geological Society, London*, **158**, 445–460.

BUCHAN, C., PFÄNDER, J. & KRÖNER, A. ET AL. 2002. Timing of accretion and collisional deformation in the Central Asian Orogenic Belt: implications of granite geochronology in the Bayankhongor Ophiolite Zone. *Chemical Geology*, **192**, 23–45.

BUSLOV, M.M., SAPHONOVA, I.YU. & WATANABE, T. ET AL. 2001. Evolution of the Paleo-Asian Ocean (Altai-Sayan Region, Central Asia) and collisions of possible Gondwana-derived terranes with the southern marginal part of the Siberian continent. *Geosciences Journal*, **5**, 203–224.

CHURCH, W.R. 1977. The ophiolites of southern Quebec: oceanic crust of Betts Cove type. *Canadian Journal of Earth Sciences*, **14**, 1668–1673.

CHURCH, W.R. 1979. The ophiolites of southern Quebec: oceanic crust of Betts Cove type: Reply. *Canadian Journal of Earth Sciences*, **16**, 1306–1308.

CHURCH, W.R. & RICCIO, L. 1977. Fractionation trends in the Bay of Islands Ophiolite of Newfoundland: polycyclic cumulate sequences in ophiolites and their classification. *Canadian Journal of Earth Sciences*, **14**, 1156–1165.

COLEMAN, R.G. 1984. The diversity of ophiolites. *Geologie en Mijnbouw*, **63**, 141–150.

COOGAN, L.A., BANKS, G.J., GILLIS, K.M., MACLEOD, C.J. & PEARCE, J.A. 2003. Hidden melt signatures recorded in the Troodos ophiolite plutonic suite: evidence for widespread generation of depleted melts and intra-crustal melt aggregation. *Contributions to Mineralogy and Petrology*, **144**, 484–506.

CUNNINGHAM, W.D., WINDLEY, B.F., DORJNAMJAA, D., BADAMGAROV, G. & SANDAAR, M. 1996. A structural transect across the Mongolian Western Altai: active transpressional mountain building in Central Asia. *Tectonics*, **15**, 142–156.

CUNNINGHAM, W.D., DAVIES, S. & BADARCH, G. 2003. Crustal architecture and active growth of the Sutai Range, western Mongolia: a major intracontinental, intraplate restraining bend. *Journal of Geodynamics*, **36**, 169–191.

DORJNAMJAA, D., BADARCH, G., BADAMGARAV, J., BAT-IREEDUI, YA., WINDLEY, B.F., CUNNINGHAM, D. & BUCHAN, C. 1998. *Geotectonic Maps of Mongolia*. Mongolian Academy of Sciences, Palaeontological Centre, Ulaanbaatar.

ELTHON, D. 1991. Geochemical evidence for formation of the Bay of Island ophiolite above a subduction zone. *Nature*, **354**, 140–142.

ENGLAND, R.N. & DAVIES, H.L. 1973. Mineralogy of ultramafic cumulates and tectonites from eastern Papua. *Earth and Planetary Science Letters*, **17**,

410–423.

GIRARDEAU, J., MERCIER, J.C.C. & TANG, Y. 1986. Petrology of the Donqiao–Xainxa Ophiolite (North Tibet): evidence for its formation in a supra-subduction zone environment. *Ofioliti*, **11**, 235–262.

GRISELIN, M. 2001. *Geochemical and isotopic study of the Xigaze and Luobusa Ophiolite Massifs (Yarlung Zangbo Suture Zone, Southern Tibet): implications for mantle partial melting and dynamic evolution of the Neo-Tethys Ocean*. Doctoral dissertation, Vrije Universiteit Amsterdam.

HAURI, E.H., WAGNER, T.P. & GROVE, T.L. 1994. Experimental and natural partitioning of Th, U, Pb and other trace elements between garnet, clinopyroxene and basaltic melts. *Chemical Geology*, **117**, 149–166.

HAWKINS, J.W. & EVANS, C.A. 1983. Geology of the Zambales Range, Luzon, Philippine Island: ophiolite from an island arc–back arc basin pair. *In:* HAYES, D. (ed.) *The Tectonic and Geologic Evolution of Southeast Asian Seas and Islands, Part 2*. American Geophysical Union, Geophysical Monograph, **27**, 95–123.

HICKEY, R.L. & FREY, F.A. 1982. Geochemical characteristics of boninite series volcanics: implications for their source. *Geochimica et Cosmochimica Acta*, **46**, 2099–2115.

HOWARD, J.P., CUNNINGHAM, W.D., DAVIES, S.J., DIJKSTRA, A.H. & BADARCH, G. 2003. The stratigraphic and structural evolution of the Dzereg Basin, Western Mongolia: clastic sedimentation, fault inversion and basin destruction in an intracontinental transpressional setting. *Basin Research*, **15**, 45–72.

ISHIKAWA, T., NAGAISHI, K. & UMINO, S. 2002. Boninitic volcanism in the Oman ophiolite: implications for thermal condition during transitions from spreading ridge to arc. *Geology*, **30**, 899–902.

JACKSON, E.D., GREEN, H.W. II & MOORES, E.M. 1975. The Vourinos Ophiolite, Greece: cyclic units of lineated cumulates overlying harzburgites tectonite. *Geological Society of America Bulletin*, **86**, 390–398.

KHAIN, YE.V. 1989. Granite–gneiss domes and ultramafic–mafic intrusions in ophiolite obduction zones. *Geotectonics*, **23**, 410–419.

KHAIN, E.V., BIBIKOVA, E.V. & SALNIKOVA, E.B. ET AL. 2003. The Palaeo-Asian ocean in the Neoproterozoic and early Palaeozoic: new geochronological data and palaeotectonic reconstructions. *Precambrian Research*, **122**, 329–358.

KLEIN, E.M. & KARSTEN, J.L. 1995. Ocean-ridge basalts with convergent-margin geochemical affinities from the Chile Ridge. *Nature*, **374**, 52–57.

KOZAKOV, I.K., SAL'NIKOVA, E.B., KHAIN, E.V., KOVACH, V.P., BEREZHNAYA, N.G., YAKOVLEVA, S.Z. & PLOTKINA, YU.V. 2002. Early Caledonian crystalline rocks of the Lake Zone in Mongolia: formation history and tectonic settings as deduced from U–Pb and Sm–Nd datings. *Geotectonics*, **36**, 156–166.

KRÖNER, A., TOMURTOGOO, O., BADARCH, G., WINDLEY, B.F. & KOZAKOV, I.K. 2001. New zircon ages and significance for crustal evolution in Mongolia. *In:* SKLYARIV, E.V. (ed.) *Assembly and Break-up of Rodinia Supercontinent: Evidence from South Siberia. Guidebook and Abstract Volume, Workshop IGCP-440, Irkutsk*. 142–145.

KUNO, H. 1968. Differentiation of basalt magmas. *In:* HESS, H.H. & POLDERVAART, A.A. (eds) *Basalts: The Poldervaart Treatise on Rocks of Basaltic Composition*. Interscience, New York, 623–688.

LUDWIG, K.R. 2001a. *User's Manual for Isoplot/Ex Rev. 2.49: a Geochronological Toolkit for Microsoft Excel*. Berkeley Geochronology Center Special Publications, **1a**.

LUDWIG, K.R. 2001b. *SQUID 1.02: a User's Manual*. Berkeley Geochronology Center Special Publications, **2**.

MACLEOD, C.J. & YAOUANCQ, G. 2000. A fossil melt lens in the Oman ophiolite: implications for magma chamber processes at fast spreading ridges. *Earth and Planetary Science Letters*, **176**, 357–373.

MAKARYCHEV, G.I., PALEY, I.P., GES', M.D., MORKOVKINA, V.F. & BURASHNIKOV, V.V. 1986. The Precambrian Rise of the Daribi Range and its significance in the structure of Western Mongolia. *Geotectonics*, **20**, 48–57.

MASON, P.R.D., JARVIS, K.E., DOWNES, H. & VANNUCCI, R. 1999. Determination of incompatible trace elements in mantle clinopyroxenes by LA-ICP-MS: a comparison of analytical performance with established techniques. *Geostandards Newsletter*, **23**, 157–173.

MATSUMOTO, I. & TOMURTOGOO, O. 2003. Petrological characteristics of the Hantaishir Ophiolite Complex, Altai Region, Mongolia: coexistence of podiform chromitite and boninite. *Gondwana Research*, **6**, 161–169.

MCDONOUGH, W. & SUN, S.-S. 1995. The composition of the Earth. *Chemical Geology*, **120**, 223–253.

MCKENZIE, D. & O'NIONS, R.K. 1991. Partial melt distributions from inversion of rare earth element concentrations. *Journal of Petrology*, **32**, 1021–1091.

METCALF, R.V., WALLIN, E.T., WILLSE, K.R. & MULLER, E.R. 2000. Geology and geochemistry of the ophiolitic Trinity terrane, California: evidence of middle Paleozoic depleted supra-subduction zone magmatism in a proto-arc setting. *In:* DILEK, Y., MOORES, E.M., ELTHON, D. & NICOLAS, A. (eds) *Ophiolites and Oceanic Crust: New Insights from Field Studies and the Ocean Drilling*

Program. Geological Society of America, Special Papers, **349**, 403–418.

MILSOM, J. 2003. Forearc ophiolites: a view from the western Pacific. *In:* DILEK, Y. & ROBINSON, P.T. (eds) *Ophiolites in Earth History*. Geological Society, London, Special Publications, **218**, 507–515.

MIYASHIRO, A. 1973. The Troodos ophiolitic complex was probably formed in an island arc. *Earth and Planetary Science Letters*, **19**, 218–224.

MIYASHIRO, A. 1975. Classification, characteristics, and origin of ophiolites. *Journal of Geology*, **83**, 249–281.

MONNIER, C., GIRARDEAU, J., MAURY, R.C. & COTTON, J. 1995. Back-arc basin origin for the East Sulawesi Ophiolite (eastern Indonesia). *Geology*, **23**, 851–854.

NAVON, O. & STOLPER, E. 1987. Geochemical consequences of melt percolation: the upper mantle as a chromatographic column. *Journal of Geology*, **95**, 285–307.

NICOLAS, A. 1989. *Structure of Ophiolites and Dynamics of Oceanic Lithosphere*. Kluwer Academic, Dordrecht.

NOIRET, G., MONTIGNY, R. & ALLÈGRE, C.J. 1981. Is the Vourinos Complex and island arc ophiolite? *Earth and Planetary Science Letters*, **56**, 375–386.

OHARA, Y., STERN, R.J., ISHII, T., YURIMOTO, H. & YAMAZAKI, T. 2002. Peridotites from the Mariana Trough: first look at the mantle beneath an active back-arc basin. *Contributions to Mineralogy and Petrology*, **143**, 1–18.

OHARA, Y., FUJIOKA, K., ISHII, R. & YURIMOTO, H. 2003. Peridotites and gabbros from the Parece Vela backarc basin: unique tectonic window in an extinct backarc spreading ridge. *Geochemistry, Geophysics, Geosystems*, **4**(7), 86111, doi:10.1029/2002GC000469.

PARKINSON, I.J. & PEARCE, J.A. 1998. Peridotites from the Izu–Bonin–Mariana Forearc (ODP Leg 125): Evidence for Mantle Melting and Melt-Mantle Interaction in a Supra-Subduction Zone Setting. *Journal of Petrology*, **39**, 1577–1618.

PEARCE, J.A., ALABASTER, T., SHELTON, A.W. & SEARLE, M.P. 1981. The Oman ophiolite as a Cretaceous arc–basin complex: evidence and implications. *Philosophical Transactions of the Royal Society of London, Series A*, **300**, 299–317.

PFÄNDER, J.A., JOCHUM, K.P., KOZAKOV, I., KRÖNER, A. & TODT, W. 2002. Coupled evolution of back-arc and island arc-like mafic crust in the late-Neoproterozoic Agardagh Tes–Chem ophiolite, Central Asia: evidence from trace element and Sr–Nd–Pb isotope data. *Contributions to Mineralogy and Petrology*, **143**, 154–174.

SACCANI, E. & PHOTIADES, A. 2004. Mid-ocean ridge and supra-subduction affinities in the Pindos ophilolites (Greece): implications for magma genesis in a fore-arc setting. *Lithos*, **73**, 229–253.

SCHROETTER, J.-M., PAGÉ, P., BÉDARD, J.H., TREMBLAY, A. & BÉCU, V. 2003. *In:* DILEK, Y. & ROBINSON, P.T. (eds) *Ophiolites in Earth History*. Geological Society, London, Special Publications, **218**, 231–251.

SENGÖR, A.M.C., NATAL'IN, B.A. & BURTMAN, V.S. 1993. Evolution of the Altaid tectonic collage and Palaeozoic crustal growth in Eurasia. *Nature*, **364**, 299–307.

SENGÖR, A.M.C., NATAL'IN, B.A. & BURTMAN, V.S. 1994. Tectonic evolution of Altaides. *Russian Geology and Geophysics*, **35**, 33–47.

SUN, S.S. & MCDONOUGH, W.F. 1989. Chemical and isotopic systematics of oceanic basalts: implications for mantle composition and processes. *In:* SAUNDERS, A.D. & NORRY, M.J. (eds) *Magmatism in the Ocean Basins*. Geological Society, London, Special Publications, **42**, 313–345.

TAYLOR, R.N., MURTON, B.J. & NESBITT, R.W. 1992. Chemical transects across intra-oceanic arcs: implications for the tectonic setting of ophiolites. *In:* PARSON, L.M., MURTON, B.J. & BROWNING, P. (eds) *Ophiolites and their Modern Oceanic Analogues*. Geological Society, London, Special Publications, **60**, 117–132.

TAYLOR, R.N., NESBITT, R.W., VIDAL, P., HARMON, R.S., AUVRAY, B. & CROUDACE, I. 1994. Mineralogy, chemistry, and genesis of the boninite series volcanics, Chichijima, Bonin Islands, Japan. *Journal of Petrology*, **35**, 577–617.

VARFALVY, V., HÉBERT, R. & BÉDARD, J.H. 1996. Interactions between melt and upper-mantle peridotites in the North Arm Mountain massif, Bay of Islands Ophiolite, Newfoundland, Canada: implications for the genesis of boninitic and related magmas. *Chemical Geology*, **129**, 71–90.

WOOD, B.J. & BLUNDY, J.D. 1997. A predictive model for rare earth element partitioning between clinopyroxene and anhydrous silicate melt. *Contributions to Mineralogy and Petrology*, **129**, 166–181.

WOODHEAD, J.D., EGGINS, S.M. & JOHNSON, R.W. 1998. Magma genesis in the New Britain Island Arc: further insights into melting and mass transfer processes. *Journal of Petrology*, **39**, 1641–1668.

ZONENSHAIN, L.P. & KUZMIN, M.I. 1978. The Khan-Taishir ophiolitic complex of western Mongolia, its petrology, origin and comparison with other ophiolitic complexes. *Contributions to Mineralogy and Petrology*, **67**, 95–109.